Nucleation in scale-free networks

Hanshuang Chen,[1] Chuansheng Shen,[1,2] Zhonghuai Hou,[1,*] and Houwen Xin[1]
[1]*Hefei National Laboratory for Physical Sciences at Microscales and Department of Chemical Physics, University of Science and Technology of China, Hefei, 230026, China*
[2]*Department of Physics, Anqing Teachers College, Anqing 246011, China*
(Received 30 April 2010; revised manuscript received 16 August 2010; published 10 March 2011)

We have studied nucleation dynamics of the Ising model in scale-free networks whose degree distribution follows a power law with the exponent γ by using the forward flux sampling method and focusing on how the network topology would influence the nucleation rate and pathway. For homogeneous nucleation, the new phase clusters grow from those nodes with smaller degree, while the cluster sizes follow a power-law distribution. Interestingly, we find that the nucleation rate R_{Hom} decays exponentially with network size and, accordingly, the critical nucleus size increases linearly with network size, implying that homogeneous nucleation is not relevant in the thermodynamic limit. These observations are robust to the change of γ and are also present in random networks. In addition, we have also studied the dynamics of heterogeneous nucleation, wherein w impurities are initially added either to randomly selected nodes or to targeted ones with the largest degrees. We find that targeted impurities can enhance the nucleation rate R_{Het} much more sharply than random ones. Moreover, $\ln(R_{\mathrm{Het}}/R_{\mathrm{Hom}})$ scales as $w^{(\gamma-2)/(\gamma-1)}$ and w for targeted and random impurities, respectively. A simple mean-field analysis is also present to qualitatively illustrate the above simulation results.

DOI: 10.1103/PhysRevE.83.031110 PACS number(s): 05.50.+q, 89.75.Hc, 64.60.Q−

I. INTRODUCTION

Complex networks describe not only the pattern discovered ubiquitously in the real world, but also provide a unified theoretical framework to understand the inherent complexity in nature [1–4]. Many real networks, as diverse as ranging from social networks to biological networks to communication networks, have been found to be scale-free [5]; that is, their degree distributions follow a power law $P(k) \sim k^{-\gamma}$. A central topic in this field has been how the network topology would influence the dynamics taking place on it. Very recently, critical phenomena in scale-free networks (SFNs) have attracted considerable research interest [6]. Examples of such phenomena include order-disorder transitions [7–11], percolation [12–15], epidemic spreading [16], synchronization [17,18], self-organized criticality [19,20], nonequilibrium pattern formation [21], and so on. These studies have revealed that network heterogeneity, characterized by diverse degree distributions, makes the critical behavior of SFNs quite different from that on regular lattices. Most previous studies focused on evaluating the onset of phase transitions in different network models. However, little attention is paid to the dynamics or kinetics of phase transitions, such as nucleation and phase separation in complex networks.

Nucleation is a fluctuation-driven process that initiates the decay of a metastable state into a more stable one [22]. A first-order phase transition usually involves the nucleation and growth of a new phase. Many important phenomena in nature, including crystallization [23], glass formation [24], and protein folding [25], are associated with nucleation. Despite its apparent importance, many aspects of nucleation processes are still unclear and deserve more investigation. The Ising model, which is a paradigm for many phenomena in statistical physics, has been widely used to study the nucleation process. Despite its simplicity, the Ising model has made important contributions to the understanding of nucleation phenomena in equilibrium systems and is also likely to yield important insights for nonequilibrium systems. In two-dimensional lattices, for instance, shear can enhance the nucleation rate and, at an intermediate shear rate the nucleate-rate peaks [26], a single impurity may considerably enhance the nucleation rate [27], and the existence of a pore may lead to two-stage nucleation and the overall nucleation rate can reach a maximum level at an intermediate pore size [28]. The nucleation pathway of the Ising model in a three-dimensional lattice has also been studied using the transition path sampling approach [29]. In addition, the Ising model has been frequently used to test the validity of classical nucleation theory (CNT) [30–34]. However, all these studies are limited to regular lattices in Euclidean space. Since many real systems can be properly modeled by complex networks, it is thus natural to ask how the topology of a networked system would influence the nucleation process of the Ising model.

Although the main motivation of the present study is to address a fundamental problem in statistical physics, it may also be of practical interest. Our study helps to understand some interesting phenomena in social networks and biological networks. This depends on the fact that, on the one hand, there is an enormous amount of research into social and biological problems that employs the Ising model and its variants [35,36]. In the social context, binary spins in the Ising model can represent two opposite opinions, or competitive language features, and the concept of physical temperature corresponds to a measure of noise due to imperfect information or uncertainty on the part of the agent, and the external field imitates the effect of mass media, yielding a bias of the agents in favor of either state [37]. In the biological context, the two states of the Ising model may correspond to a neuron being fired or not or a gene being on or off. Furthermore, physical temperature can be interpreted

*hzhlj@ustc.edu.cn

as stochastic fluctuations at the cellular level, and the external field naturally represents external stimuli. On the other hand, our study may be relevant to some known phenomena observed in the literature. These phenomena usually involve fluctuation-driven transition processes in collective behavior. For instance, Dasgupta *et al.* found the coexistence of two distinct phases in the Ising model of a modular network—modular order and global order—and showed that the transition from modular order to global order corresponds to consensus formation in social networks [38]. Similar phenomena have also been observed in the Ising model of two coupled scale-free networks by Suchecki *et al.* [39] and, in the opinion model, of two coupled random networks by Lambiotte *et al.* [40]. How one language that is spoken by everybody can be replaced by another language is another example in social science related to the present study, which has been studied by empirical data and computer simulation in lattice [41] and complex networks [42,43], suggesting that population size plays a vital role in determining the change rate. In addition, there are many examples about functional transition in biological networks such as the transition between different dynamical attractors in neural networks [44] and the genetic switch between high- and low-expression states in gene regulatory networks [45,46].

In the present work, we have studied the nucleation process of the Ising model in SFNs. Since nucleation is an activated process that occurs extremely slowly, brute-force simulation is prohibitively expensive. To overcome this difficulty, we adopt a recently developed forward flux sampling (FFS) method to obtain the rate and pathway for nucleation [47]. For homogeneous nucleation, we find that the nucleation begins with nodes with smaller degree, while nodes with larger degree are more stable. We show that the nucleation rate decays exponentially with network size N and, accordingly, the critical nucleus size increases linearly with N, implying that homogeneous nucleation can only occur in finite-size networks. Comparing the results of networks with different γ and those of random networks, we conclude that network heterogeneity is unfavorable to nucleation. In addition, we have also investigated heterogeneous nucleation by adding impurities into the networks. It is found that the dependence of the nucleation rate on the number of random impurities is significantly different from the case of targeted impurities. These simulation results may be qualitatively understood in a mean-field (MF) manner.

The rest of the paper is organized as follows. In Sec. II, we give the details of our simulation model and the FFS method applied to this system. In Sec. III, we present the results for the nucleation rate and pathway. We then show, via both simulation and analysis, the system-size effect of the nucleation rate and heterogeneous nucleation. At last, the discussion and main conclusions are addressed in Sec. IV.

II. MODEL AND SIMULATION DETAILS

A. Networked Ising model

The Ising model in a network comprised of N nodes is described by the Hamiltonian

$$H = -J \sum_{i<j} a_{ij} s_i s_j - h \sum_i s_i, \tag{1}$$

where the spin variable s_i at node i takes either $+1$ (up) or -1 (down). $J(>0)$ is the coupling constant and h is the external magnetic field. The elements of the adjacency matrix of the network take $a_{ij} = 1$ if nodes i and j are connected and 0 otherwise.

Our simulation is performed by Metropolis spin-flip dynamics [48], in which we attempt to flip each spin once, on average, during each Monte Carlo (MC) cycle. In each attempt, a randomly chosen spin is flipped with the probability $\min(1, e^{-\beta \Delta E})$, where $\beta = 1/(k_B T)$ with k_B being the Boltzmann constant and T the temperature, and ΔE is the energy change due to the flipping process. Generally, with the increment of T, the system will undergo a second-order phase transition at the critical temperature T_c from an ordered state to a disordered one [7–11]. To study nucleation, we set $J = 1$, $h > 0$, $T < T_c$, and start from a metastable state in which $s_i = -1$ for most of the spins. The system will stay in that state for a significantly long time before undergoing a nucleation transition to the thermodynamic stable state with most spins pointing up. We are interested in dynamics of this nucleation process.

B. Forward flux sampling

The FFS method has been used to calculate rate constants, transition paths, and stationary probability distributions for rare events in equilibrium and nonequilibrium systems [26–28,47,49,50]. This method uses a series of interfaces in phase space between the initial and final states to force the system from the initial state A to the final state B in a ratchet-like manner. An order parameter $\lambda(x)$ is first defined, where x represents the phase-space coordinates, such that the system is in state A if $\lambda(x) < \lambda_0$ and state B if $\lambda(x) > \lambda_m$, while a series of nonintersecting interfaces λ_i $(0 < i < m)$ lie between states A and B, such that any path from A to B must cross each interface without reaching λ_{i+1} before λ_i. The transition rate R from A to B is calculated as

$$R = \bar{\Phi}_{A,0} P(\lambda_m | \lambda_0) = \bar{\Phi}_{A,0} \prod_{i=0}^{m-1} P(\lambda_{i+1} | \lambda_i), \tag{2}$$

where $\bar{\Phi}_{A,0}$ is the average flux of trajectories crossing λ_0 in the direction of B. $P(\lambda_m|\lambda_0) = \prod_{i=0}^{m-1} P(\lambda_{i+1}|\lambda_i)$ is the probability that a trajectory crossing λ_0 in the direction of B will eventually reach B before returning to A, and $P(\lambda_{i+1}|\lambda_i)$ is the probability that a trajectory which reaches λ_i, having come from A, will reach λ_{i+1} before returning to A. For more information about FFS, please turn to Ref. [51].

III. RESULTS

A. Homogeneous nucleation: rate and pathway

To begin with, we consider homogeneous nucleation in a Barabási-Albert–scale-free network (BA-SFN), whose degree distribution follows a power law $P(k) \sim k^{-\gamma}$ with the scaling exponent $\gamma = 3$ [5]. We define the order parameter λ as the total number of up spins in the networks. We set $N = 1000$, the average degree $\langle k \rangle = 6$, $T = 2.59$, $h = 0.7$, $\lambda_0 = 130$, and $\lambda_m = 880$, where T is lower than the critical temperature $T_c \simeq 10.36$. The spacing between interfaces is fixed at

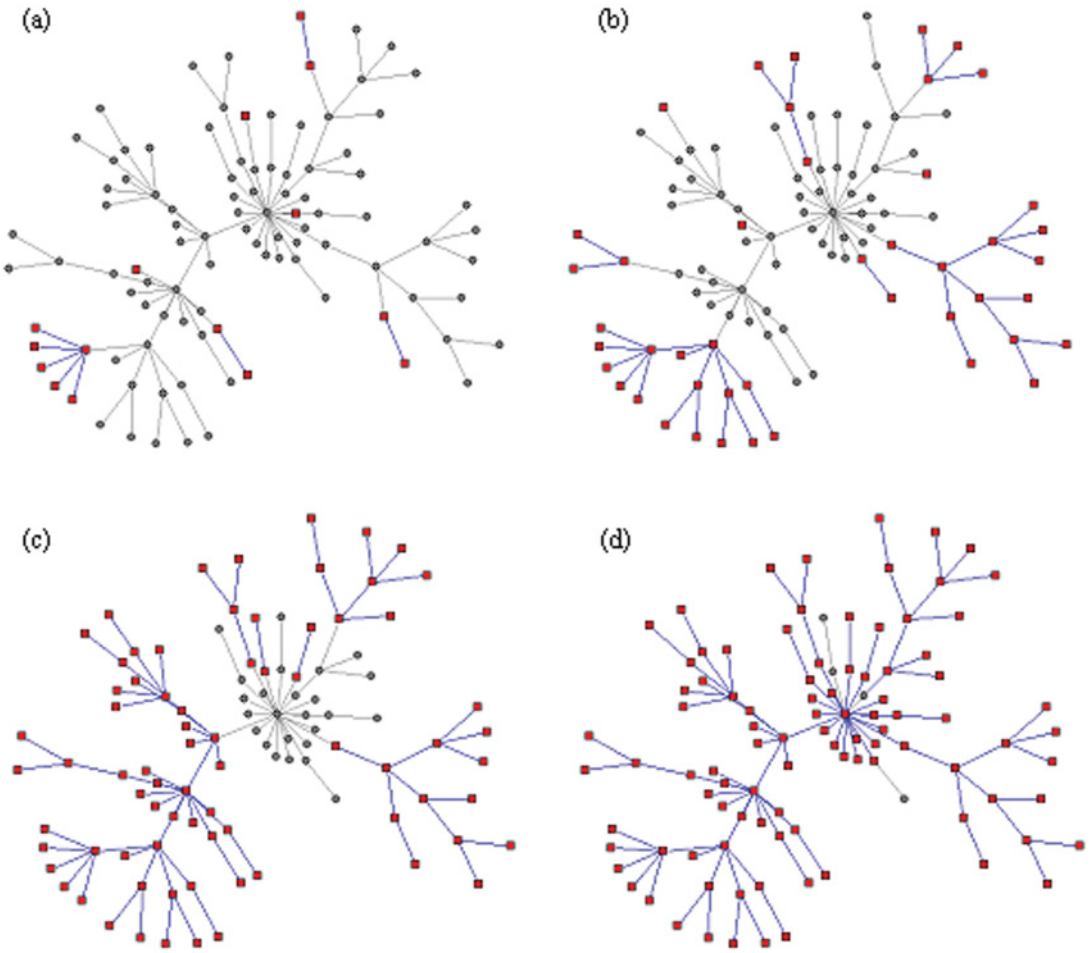

FIG. 1. (Color online) Snapshots of nucleation in a BA scale-free network with $N = 100$ and $\langle k \rangle = 2$ at four different stages. Up spins and down spins are indicated by red squares and black circles, respectively.

3 up spins, but the computed results do not depend on this spacing. During the FFS sampling, we perform 1000 trials at each interface, from which at least 100 configurations are stored in order to investigate the statistical properties of the ensemble of nucleation pathways. We obtain $\bar{\Phi}_{A,0} = 1.24 \times 10^{-4}\,\mathrm{MC\,step^{-1}spin^{-1}}$ and $P(\lambda_m|\lambda_0) = 4.48 \times 10^{-46}$, resulting in $R_{\mathrm{Hom}} = 5.55 \times 10^{-50}\,\mathrm{MC\,step^{-1}spin^{-1}}$ following Eq. (2). Such a nucleation rate is very low such that a brute-force simulation would be very expensive.

From the stored configurations at each interface, one can figure out the details of the nucleation pathway. Figure 1 illustrates schematically four stages of a typical nucleation pathway. Clearly, the new phase (indicated by squares) starts from nodes with smaller degrees, while nodes with larger degrees are more stable. This picture is reasonable because flipping nodes with larger degrees requires overcoming more interfacial energies. Figure 2(a) plots the average degree of nodes in the new phase, $\langle k_{\mathrm{new}} \rangle$, as a function of the order parameter λ. As expected, $\langle k_{\mathrm{new}} \rangle$ increases monotonically with λ. On the other hand, it is observed that the formation of large clusters of new phase is accompanied with the growth and coalescence of small clusters. Interestingly, we find that the size N_c of new-phase clusters follows a power-law distribution at the early stages of nucleation: $P(N_c) \sim N_c^{-\alpha}$ with the fitting exponent $\alpha \simeq 2.44$, as shown in Fig. 2(b). With the emergence of a giant component of new phase, the tail of the distribution is elevated, but the size distribution for the remaining clusters still follows a power law. The underlying mechanism of such a phenomenon is still an open question for us.

To determine the critical size λ_c of the nucleus we compute the committor probability P_B, which is the probability of reaching the thermodynamic stable state before returning to the metastable state. The dependence of P_B on λ is plotted in Fig. 3(a). As commonly reported in the literature [29,34], the critical nucleus appears at $P_B(\lambda_c) = 0.5$, giving the critical nucleus size $\lambda_c^{\mathrm{FFS}} = 474$. The committor distribution at λ_c^{FFS} exhibits a peak at 0.5, for which 70% of spin configurations have P_B values within the range of 0.4 to 0.6 [see the inset of Fig. 3(a)], indicating that λ is a proper order parameter.

Note that, conventionally, the nucleation threshold λ_c is usually estimated by using CNT [52–54]. One can calculate the free-energy change along the nucleation path, $\Delta F(\lambda)$, by using methods like umbrella sampling (US) [55]. According to CNT, ΔF will bypass a maximum at $\lambda = \lambda_c^{\mathrm{US}}$, and the nucleation rate is given by $\nu \exp(-\beta \Delta F_c)$, where ν is an attempt frequency. Here we have computed ΔF by using US, in which we have adopted a bias potential $0.1 k_B T(\lambda - \bar{\lambda})^2$, with $\bar{\lambda}$ being the center of each window. As shown in Fig. 3(b),

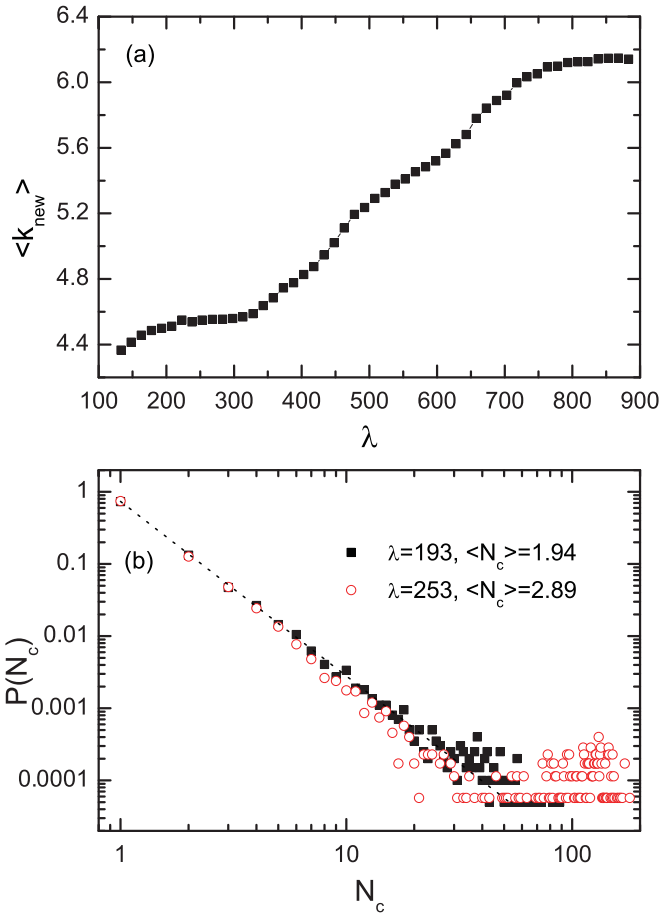

FIG. 2. (Color online) (a) Average degree of nodes of new phase $\langle k_{\rm new}\rangle$ as a function of λ; (b) Size distribution of clusters of new phase, in which a power-law distribution is present. Other parameters are $N = 1000$, $\langle k\rangle = 6$, $T = 2.59$, and $h = 0.7$.

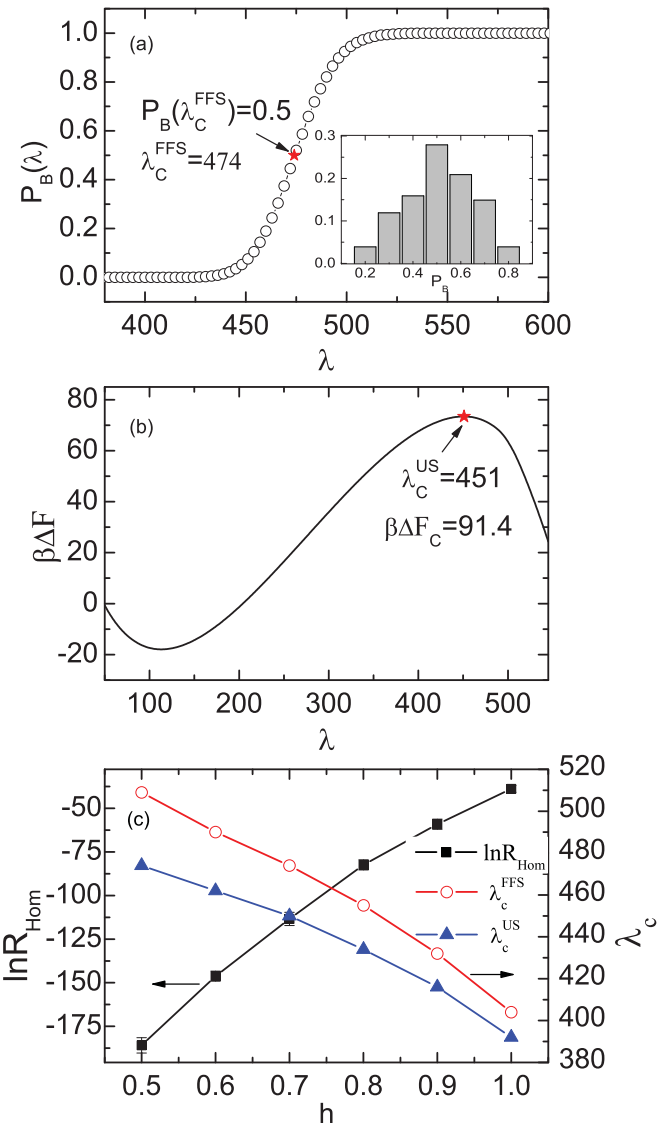

FIG. 3. (Color online) (a) Committor probability P_B as a function of λ; the inset plots the committor distribution at $\lambda_c^{\rm FFS}$. (b) Free energy ΔF as a function of λ, in which the maximum in ΔF occurs at $\lambda_c^{\rm US}$. (c) Logarithm of homogeneous nucleation rate $\ln R_{\rm Hom}$ (left axis), and the critical size of nucleus, $\lambda_c^{\rm FFS}$ and $\lambda_c^{\rm US}$ (right axis), obtained by the FFS method and US method, respectively, as functions of h. Other parameters are the same as for Fig. 2.

the maximum in ΔF occurs at $\lambda_c^{\rm US} = 451$, giving a free-energy barrier of $\Delta F_c \simeq 91.4 k_B T$. Clearly, $\lambda_c^{\rm US}$ gives a fairly good estimation of $\lambda_c^{\rm FFS}$. To calculate the nucleation rate, however, one has to obtain the attempt frequency ν, which is not a trivial task. If we just set $\nu = 1$, we obtain a CNT prediction of a rate of 2.02×10^{-40} MC step^{-1}spin^{-1}, which is 9 orders of magnitude faster than that computed by the FFS method. This level of disagreement in nucleation rate corresponds to an error in the free-energy barrier of about 24%. Since the accurate value of ν is generally unavailable, we will use the FFS method to calculate the nucleation rate throughout this paper. In addition, the real nucleation pathway cannot be obtained by the conventional US method due to the use of a biased potential.

We have also investigated how the nucleation rate and threshold depend on the external field h. In Fig. 3(c), $\ln R_{\rm Hom}$, $\lambda_c^{\rm FFS}$, and $\lambda_c^{\rm US}$ are plotted as functions of h. The error bars are obtained via 20 different network realizations and 10 independent FFS samplings. As expected, $\ln R_{\rm Hom}$ increases monotonically with h, and $\lambda_c^{\rm FFS}$ and $\lambda_c^{\rm US}$ both decrease with h. For large h, the difference between $\lambda_c^{\rm FFS}$ and $\lambda_c^{\rm US}$ becomes small. If h is large enough, one expects that the free-energy barrier will disappear, and nucleation will not be relevant.

To check the generality of the above results, we have also considered homogeneous nucleation in many other network models, such as SFNs with other scaling exponents γ and the well-known Erdös-Rényi random network. The networks are generated according to the Molloy-Reed model [56]: Each node is assigned a random number of stubs k that are drawn from a specified degree distribution. This construction eliminates the degree correlations between neighboring nodes. Extensive simulations have shown that the qualitative results of Figs. 1–3 hold for all the network models under study: (i) Nucleation starts from nodes, on average, with smaller degrees, and the sizes of clusters of nucleating phase are power-law distributed but with slightly different exponents for different networks. (ii) By comparing the nucleation rate

$R_{\rm Hom}$ and the size of critical nucleus λ_c, obtained by the FFS and US methods, we found that they are approximately in agreement. However, for different network models, $R_{\rm Hom}$ and λ_c are quantitatively different for the same system parameters, and the comparison will be made in the subsequent part, suggesting that degree heterogeneity plays an important role. (iii) We have also examined the dependence of $R_{\rm Hom}$ and λ_c on the external field h and found that the same trends as in Fig. 3(c) are also present.

B. Homogeneous nucleation: system-size effects

According to Fig. 3, one finds that nearly half of the nodes must be inverted to achieve nucleation. This means that, for a large network, nucleation occurs with great difficulty. An interesting question thus arises: How do the nucleation rate and threshold depend on the network size?

To answer this question, we have performed extensive simulations to calculate $R_{\rm Hom}$ and λ_c for different network size N. In particular, besides the BA-SFNs, we have also considered different network types, including SFNs with other scaling exponents γ and homogeneous random networks (HoRNs) [57]. We note here that the exponent γ can be a measure of degree heterogeneity of the network; that is, the smaller γ is, the more heterogeneous is the degree distribution. In a HoRN, each node is equivalently connected to $\langle k\rangle$ other nodes, randomly selected from the whole network, such that no degree heterogeneity exists. By comparing the results in SFNs with different γ as well as that in HoRNs, one can, on the one hand, check the robustness of the system size effects and, on the other hand, investigate how the degree heterogeneity affects the nucleation process.

Figure 4 shows the simulation results. All the parameters are the same as in Fig. 2, expect that N varies from $N = 500$ to $N = 3000$. Interestingly, both $\ln R_{\rm Hom}$ and λ_c show very good linear dependencies on the system size (i.e., $\ln R_{\rm Hom} \sim -aN$ and $\lambda_c \sim bN$ with a and b being positive constants). Obviously, in the thermodynamic limit $N \to \infty$, we have $R_{\rm Hom} \to 0$ and $\lambda_c \to \infty$. This means that nucleation in these systems is not relevant in the thermodynamic limit, and only finite-size systems are of interest. As shown in Fig. 4, for the network types considered here, qualitative behaviors are the same. Quantitatively, with increasing γ, the line slope becomes smaller, $R_{\rm Hom}$ becomes larger, and λ_c gets smaller. Since larger γ corresponds to more homogeneous degree distribution, these results indicate that the degree heterogeneity is unfavorable to nucleation. This is consistent with the nucleation pathway as shown in Fig. 2: In a heterogenous network, those hub nodes are difficult to flip, making nucleation difficult.

In the following, we will show that the system-size effects can be qualitatively understood by CNT and simple MF analysis. According to CNT, the formation of a nucleus lies in two competing factors: the energy cost of creating a new up spin which favors the growth of the nucleus, and an opposing factor which is due to the creation of new interfaces between up and down spins. The change in the free energy may be written as [52–54]

$$\Delta F(\lambda) = -2h\lambda + \sigma\lambda, \tag{3}$$

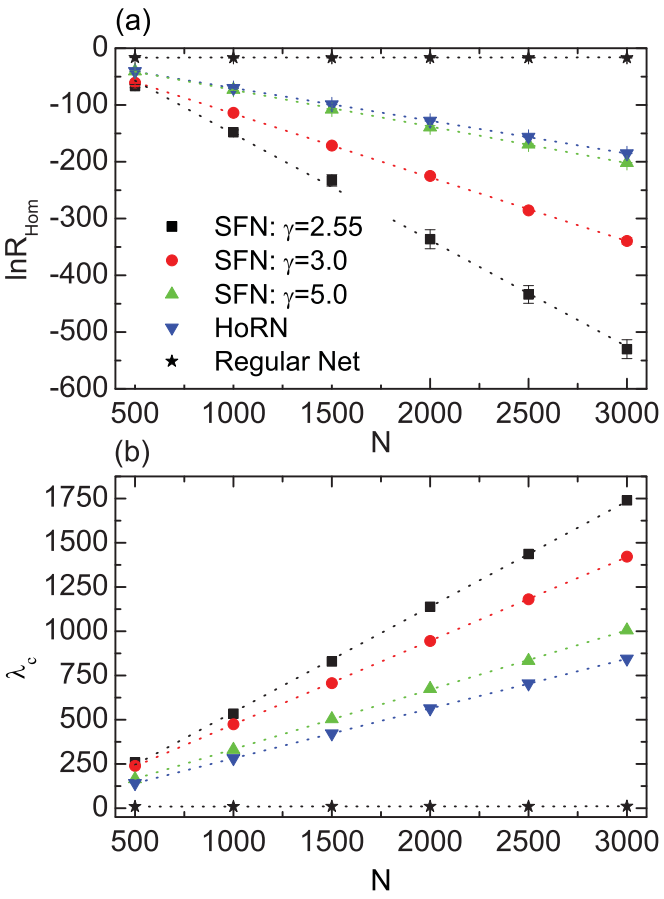

FIG. 4. (Color online) (a) Logarithm of homogeneous nucleation rate $\ln R_{\rm Hom}$ and (b) the critical size of nucleus λ_c as functions of the network size N in SFNs with different γ, HoRNs, and regular networks. For SFNs and HoRNs, other parameters are the same as for Fig. 2. For regular networks, the parameters $\langle k\rangle = 6$, $T = 1.5$, and $h = 0.1$ are used.

where σ denotes the effective interfacial free energy, which may depend on T, h, and N. Since interfacial interactions arise from up spins inside the nucleus and down spins outside of it, one may write $\sigma = 2JK_{\rm out}$ by neglecting entropy effects (zero-temperature approximation), where $K_{\rm out}$ is the average number of neighboring down-spin nodes that an up-spin node has. Using the MF approximation, one has $K_{\rm out} = \langle k\rangle(1 - \lambda/N)$. Inserting this relation into Eq. (3) and maximizing ΔF with respect to λ, we have

$$\lambda_c^{\rm MF} = \frac{J\langle k\rangle - h}{2J\langle k\rangle}N \tag{4}$$

and the free-energy barrier

$$\Delta F_c^{\rm MF} = \frac{(J\langle k\rangle - h)^2 N}{2J\langle k\rangle}. \tag{5}$$

Clearly, both $\lambda_c^{\rm MF}$ and $\Delta F_c^{\rm MF}$ increase linearly with N if other parameters are fixed. Therefore, the linear relationships shown in Fig. 4 are essentially analogous to the behavior of a mean-field network. Quantitatively, however, the MF analysis fails to predict the line slopes in Fig. 4. This can be understood because the approximations are so crude, wherein important aspects such as network heterogeneity and entropy effects have

not been taken into account. A rigid analysis is not a trivial task and is beyond the scope of the present work.

It should be pointed out that such system-size dependence does not exist in two-dimensional regular lattices [27]. We have also studied nucleation of Ising systems in regular networks where each node is connected to its k-nearest neighbors (here we only consider the case of sparse networks; that is, $k \ll N$) and found that both the rate and the size of critical nucleus are almost independent of network size (results shown in Fig. 4). Therefore, nucleation processes in SFNs and HoRNs are quite different from those in regular lattices or networks.

C. Heterogeneous nucleation

In practice, most nucleation events that occur in nature are heterogeneous (i.e., impurities of the new phase are initially present). It is well known that impurities can increase the nucleation rate by as much as several orders of magnitude. In our model, impurities are introduced by fixing some nodes in the up-spin state. We are interested in how the number w of impurity nodes and the way of adding impurities would affect the nucleation rate. The first way of adding impurities we use is that impurity nodes are selected in a random fashion. Figure 5(a) gives the simulation results of $\ln(\frac{R_{\rm Het}}{R_{\rm Hom}})$ as a function of w in different network models, where $R_{\rm Het}$ are the rates of heterogeneous nucleation. As expected, nucleation becomes faster in the presence of random impurities no matter which kind of network model is applied. It seems that, in Fig. 5(a), all data collapse and exhibit a linear dependence on w, with the fitting slope 3.33. This means that each additional random impurity can lead to the increase of the rate by more than one order of magnitude. For the second way, we select w nodes with the most high degree as the impurity nodes, termed targeted impurities. Strikingly, such a targeted scheme is much more effective in increasing the nucleation rate than a random one, as shown in Fig. 5(b). For example, for SFNs with $\gamma = 3$, one single targeted impurity can increase the rate by about 36 orders of magnitude.

As in Sec. III B, below we will also give an MF analysis of the heterogeneous nucleation, which qualitatively agrees with the simulation results. Each impurity node contributes an additional term to the free-energy barrier, which can, under the zero-temperature approximation, be written as the product of $-2J$ and the expected degree of the impurity node. For random impurities, each impurity node has an expected degree $\langle k\rangle$, yielding the term $-2J\langle k\rangle$. Thus, the resulting free-energy barrier of the heterogenous nucleation becomes $\Delta_1 F_c^{\rm Het} = \Delta F_c^{\rm Hom} - 2J\langle k\rangle w$, where $\Delta F_c^{\rm Hom}$ is the free-energy barrier of homogeneous nucleation. According to CNT, one obtains

$$\ln\left(\frac{R_{\rm Het}}{R_{\rm Hom}}\right) = \frac{2J\langle k\rangle}{k_B T} w. \tag{6}$$

Therefore, nucleation with random impurities is always faster than without impurities, and $\ln(\frac{R_{\rm Het}}{R_{\rm Hom}})$ should vary linearly with w. The theoretical estimate of the slope is given by $2J\langle k\rangle/(k_B T) = 4.63$, approximately consistent with the simulation estimate. Given the simple nature of the above approximation, the agreement is satisfactory. For the targeted way, a treatment similar to the former case can also be executed, except that $\langle k\rangle$ should be replaced by $\langle k\rangle_w$, where $\langle k\rangle_w$ is the average degree of the w targeted nodes. After simple calculations, we can obtain $\langle k\rangle_w = \langle k\rangle(\frac{N}{w})^{\frac{1}{\gamma-1}}$. This leads to

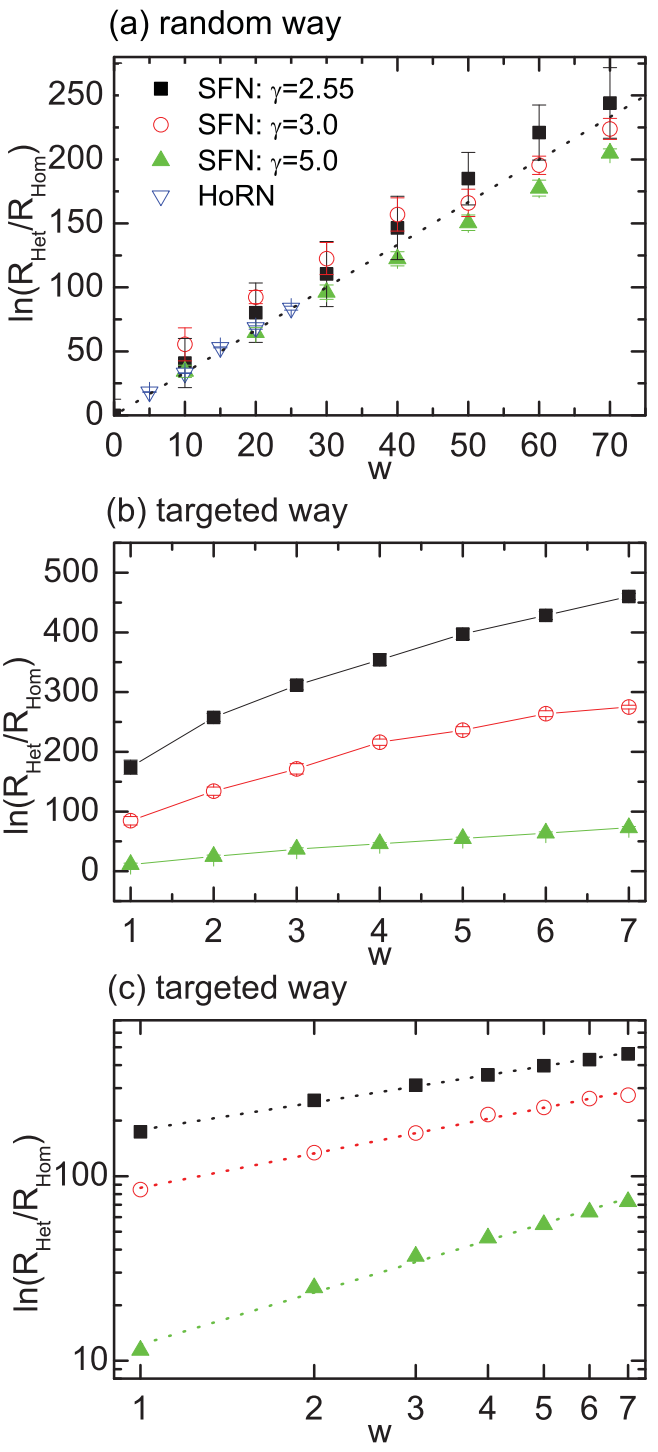

FIG. 5. (Color online) $\ln(\frac{R_{\rm Het}}{R_{\rm Hom}})$ as a function of the number of impurity nodes w. Panel (a) corresponds to the case of random impurities, while panels (b) and (c) correspond to the case of targeted impurities. Panel (c) plots $\ln(\frac{R_{\rm Het}}{R_{\rm Hom}})$ versus w in double logarithmic coordinates. All dotted lines are drawn by linear fitting. Other parameters are the same as for Fig. 2 except for $h = 0.2$.

a free-energy barrier, $\Delta_2 F_c^{\rm Het} = \Delta F_c^{\rm Hom} - 2J\langle k\rangle N^{\frac{1}{\gamma-1}} w^{\frac{\gamma-2}{\gamma-1}}$, and

$$\ln\left(\frac{R_{\rm Het}}{R_{\rm Hom}}\right) = \frac{2J\langle k\rangle}{k_B T} N^{\frac{1}{\gamma-1}} w^{\frac{\gamma-2}{\gamma-1}}. \quad (7)$$

Compared with Eq. (6) and besides the presence of an additional size-dependent factor of $N^{\frac{1}{\gamma-1}}$, the w-dependent factor becomes $w^{\frac{\gamma-2}{\gamma-1}}$ rather than w. For a homogeneous network, (i.e., $\gamma \to \infty$) one obtains $N^{\frac{1}{\gamma-1}} \to 1$ and $w^{\frac{\gamma-2}{\gamma-1}} \to w$, and Eq. (7) is thus equivalent to Eq. (6). In Fig. 5(c), we plot the simulation results of $\ln(\frac{R_{\rm Het}}{R_{\rm Hom}})$ as a function of w in double logarithmic coordinates, where linear dependencies are apparent, in agreement with the result of Eq. (7). The fitting slopes μ and intercepts κ for $\gamma = 2.55$, 3.0, and 5.0 in Fig. 5(c) are $\mu = 0.49$, 0.62, and 0.93 and $\kappa = 2.25$, 1.94, and 1.08, respectively, while our analytical estimates are $\mu = \frac{\gamma-2}{\gamma-1} = 0.35$, 0.50, and 0.75 and $\kappa = \log_{10}[2J\langle k\rangle N^{1/(\gamma-1)}/(k_B T)] = 2.60$, 2.16, and 1.42, respectively. Simulations and analysis give the same trends for μ, κ, and γ.

IV. DISCUSSION AND CONCLUSIONS

Our investigations of system-size effects of nucleation in SFNs and HoRNs have revealed that the nucleation rate is size dependent, and it decreases exponentially with the network size, resulting in nucleation occurring only for finite-size systems. However, for nucleation in regular networks the rate is independent of the network size. Such differences may originate from the infinite-dimensional properties of SFNs and HoRNs, wherein the average path distance is rather small, rendering the system's behavior analogous to that of a mean-field network. An interesting situation arises when one considers a Watts-Strogatz small-world network, which is constructed by randomly rewiring each link of a regular network with the probability p [58]. With the increment of p from 0 to 1, the resulting network changes from a regular network to a completely random one. As mentioned above, for the nucleation process no system-size effects exist for $p = 0$, while system-size dependence exists for $p = 1$. One may naturally ask: How does the crossover happens when p changes from 0 to 1, and what is the physical significance of such a transition? This question surely deserves further investigations and may be the content of a future presentation.

The size-effect of the transition rate has also been observed in language dynamical networks and bistable genetic networks. In [43], it was demonstrated by a theoretical model in BA-SFN and by empirical data that the rate of language change depends on the population size within certain parameter settings. The larger the population gets, the more slowly the language will change. In [46], it was shown that a genetic network with larger size will spend more time staying in one stable state before jumping to another one. A recent work has shown that the relaxation time of the Ising model in modular networks from a metastable state with local order to a stable state with global order decreases with an external field [38], which is qualitatively consistent with our results in Fig. 3(c). Our results of heterogeneous nucleation may have particular relevance to the work of [44], in which the response of Ising-type neural networks with two different dynamic attractors under stimuli was considered, and a key finding is that SFNs are much more sensitive than random networks in response to targeted stimuli. In a very recent paper [59], it was shown that the evolution of the coauthorship network of a new research field undergoes the nucleation of small isolated components on the early transient stages. From the present study one can expect to gain new insights into determining the transition rate and characterizing the pathway to nucleation transition in networked interacting systems.

In summary, we have studied homogeneous and heterogeneous nucleation of the Ising model in SFNs by using the FFS method. For homogeneous nucleation, we find that the formation of a new phase starts from nodes with a smaller degree, while nodes with a higher degree are more stable. Extensive simulations show that the nucleation rate decreases exponentially with the network size N and the nucleation threshold increases linearly with N, indicating that nucleation in these systems is not relevant in the thermodynamic limit. For heterogeneous nucleation, target impurities are shown to be much more efficient to enhance the nucleation rate than random ones. A simple MF analysis is also presented to qualitatively illustrate the simulation results. Our study may provide a valuable understanding of how first-order phase transitions take place in network-organized systems and how to effectively control the rate of such processes.

ACKNOWLEDGMENTS

This work is supported by the National Science Foundation of China under Grants No. 20933006 and No. 20873130. The authors thank Jesús Gómez-Gardeñnes and Dietrich Stauffer for helpful discussions.

[1] R. Albert and A.-L. Barabási, Rev. Mod. Phys. **74**, 47 (2002).
[2] S. Boccaletti, V. Latora, Y. Moreno, M. Chavez, and D.-U. Hwang, Phys. Rep. **424**, 175 (2006).
[3] A. Arenas, A. Díaz-Guilera, J. Kurths, Y. Moreno, and C. Zhou, Phys. Rep. **469**, 93 (2008).
[4] M. E. J. Newman, SIAM Rev. **45**, 167 (2003).
[5] A.-L. Barabási and R. Albert, Science **286**, 509 (1999).
[6] S. N. Dorogovtsev, A. V. Goltseve, and J. F. F. Mendes, Rev. Mod. Phys. **80**, 1275 (2008).
[7] A. Aleksiejuk, J. A. Holysta, and D. Stauffer, Physica A **310**, 260 (2002).
[8] G. Bianconi, Phys. Lett. A **303**, 166 (2002).
[9] S. N. Dorogovtsev, A. V. Goltsev, and J. F. F. Mendes, Phys. Rev. E **66**, 016104 (2002).
[10] M. Leone, A. Vázquez, A. Vespignani, and R. Zecchina, Eur. Phys. J. B **28**, 191 (2002).
[11] C. P. Herrero, Phys. Rev. E **69**, 067109 (2004).
[12] R. Cohen, K. Erez, D. ben Avraham, and S. Havlin, Phys. Rev. Lett. **85**, 4626 (2000).

[13] D. S. Callaway, M. E. J. Newman, S. H. Strogatz, and D. J. Watts, Phys. Rev. Lett. **85**, 5468 (2000).
[14] M. E. J. Newman, Phys. Rev. Lett. **89**, 208701 (2002).
[15] R. Cohen, D. ben Avraham, and S. Havlin, Phys. Rev. E **66**, 036113 (2002).
[16] R. Pastor-Satorras and A. Vespignani, Phys. Rev. Lett. **86**, 3200 (2001).
[17] T. Nishikawa, A. E. Motter, Y.-C. Lai, and F. C. Hoppensteadt, Phys. Rev. Lett. **91**, 014101 (2003).
[18] J. Gómez-Gardeñes, Y. Moreno, and A. Arenas, Phys. Rev. Lett. **98**, 034101 (2007).
[19] K. I. Goh, D.-S. Lee, B. Kahng, and D. Kim, Phys. Rev. Lett. **91**, 148701 (2003).
[20] A. E. Motter and Y. C. Lai, Phys. Rev. E **66**, 065102 (2002).
[21] H. Nakao and A. S. Mikhailov, Nat. Phys. **6**, 544 (2010).
[22] D. Kashchiev, *Nucleation: Basic Theory with Applications* (Butterworths-Heinemann, Oxford, 2000).
[23] L. Gránásy and F. Iglói, J. Chem. Phys. **107**, 3634 (1997).
[24] G. Johnson, A. I. Melćuk, H. Gould, W. Klein, and R. D. Mountain, Phys. Rev. E **57**, 5707 (1998).
[25] A. R. Fersht, Proc. Natl. Acad. Sci. USA **92**, 10869 (1995).
[26] R. J. Allen, C. Valeriani, S. Tanase-Nicola, P. R. ten Wolde, and D. Frenke, J. Chem. Phys. **129**, 134704 (2008).
[27] R. P. Sear, J. Phys. Chem. B **110**, 4985 (2006).
[28] A. J. Page and R. P. Sear, Phys. Rev. Lett. **97**, 065701 (2006).
[29] A. C. Pan and D. Chandler, J. Phys. Chem. B **108**, 19681 (2004).
[30] M. Acharyya and D. Stauffer, Eur. Phys. J. B **5**, 571 (1998).
[31] V. A. Shneidman, K. A. Jackson, and K. M. Beatty, J. Chem. Phys. **111**, 6932 (1999).
[32] S. Wonczak, R. Strey, and D. Stauffer, J. Chem. Phys. **113**, 1976 (2000).
[33] K. Brendel, G. T. Barkema, and H. van Beijeren, Phys. Rev. E **71**, 031601 (2005).
[34] S. Ryu and W. Cai, Phys. Rev. E **81**, 030601 (2010).
[35] C. Castellano, S. Fortunato, and V. Loreto, Rev. Mod. Phys. **81**, 591 (2009).
[36] J. J. Hopfield, Proc. Natl. Acad. Sci. USA **79**, 2554 (1982).
[37] D. Stauffer, Am. J. Phys. **76**, 470 (2008).
[38] S. Dasgupta, R. K. Pan, and S. Sinha, Phys. Rev. E **80**, 025101 (2009).
[39] K. Suchecki and J. A. Hołyst, Phys. Rev. E **80**, 031110 (2009).
[40] R. Lambiotte and M. Ausloos, J. Stat. Mech. (2007) P08026.
[41] D. Nettle, Lingua **108**, 119 (1999).
[42] J. Ke, T. Gong, and W. S.-Y. Wang, Comput. Phys. Commun. **3**, 935 (2008).
[43] S. Wichmann, D. Stauffer, C. Schulze, and E. W. Holman, Adv. Complex Syst. **11**, 357 (2008).
[44] Y. Bar-Yam and I. R. Epstein, Proc. Natl. Acad. Sci. USA **101**, 4341 (2004).
[45] T. Tian and K. Burrage, Proc. Natl. Acad. Sci. USA **103**, 8372 (2006).
[46] A. Koseska, A. Zaikin, J. Kurths, and J. García-Ojalvo, PLoS ONE **4**, e4872 (2009).
[47] R. J. Allen, P. B. Warren, and P. R. ten Wolde, Phys. Rev. Lett. **94**, 018104 (2005).
[48] D. P. Landau and K. Binder, *A Guide to Monte Carlo Simulations in Statistical Physics* (Cambridge University Press, Cambridge, 2000).
[49] C. Valeriani, R. J. Allen, M. J. Morelli, D. Frenkel, and P. R. ten Wolde, J. Chem. Phys. **127**, 114109 (2007).
[50] R. J. Allen, D. Frenkel, and P. R. ten Wolde, J. Chem. Phys. **124**, 024102 (2006).
[51] R. J. Allen, C. Valeriani, and P. R. ten Wolde, J. Phys. Condens. Matter **21**, 463102 (2009).
[52] R. Becker and W. Döring, Ann. Phys. (NY) **24**, 719 (1935).
[53] Y. B. Zeldovich, Ann. Phys. (NY) **18**, 1 (1943).
[54] A. Laaksonen, V. Talanquer, and D. W. Oxtoby, Annu. Rev. Phys. Chem. **46**, 489 (1995).
[55] J. S. van Duijneveldt and D. Frenkel, J. Chem. Phys. **96**, 15 (1992).
[56] M. Molloy and B. Reed, Random Struct. Algorithms **6**, 161 (1995).
[57] F. C. Santos, J. F. Rodrigues, and J. M. Pacheco, Phys. Rev. E **72**, 056128 (2005).
[58] D. J. Watts and S. H. Strogatz, Nature (London) **393**, 440 (1998).
[59] D. Lee, K. I. Goh, B. Kahng, and D. Kim, Phys. Rev. E **82**, 026112 (2010).